NUMERICAL ANALYSIS OF STRIP-SHAPED UNBONDED SCRAP TIRE RUBBER PAD ISOLATORS (SSU-STRP) UNDER MULTIDIRECTIONAL CYCLIC LOADING

Fahim Shahriar*[1], Md. Basir Zisan[2], Shakwat Karim Maher[3], Dip Narayan Yadav[4]

[1] Lecturer, Department of Civil Engineering, CUET, Bangladesh, e-mail: fahim.shahriar@cuet.ac.bd*
[2] Professor, Department of Civil Engineering, CUET, Bangladesh, e-mail: basirzisan@cuet.ac.bd
[3] Research Assistant, Department of Civil Engineering, CUET, Bangladesh, e-mail: shakwatkarim8880@gmail.com
[4] Graduate student, Department of Civil Engineering, CUET, Bangladesh, e-mail: dipyadav79@gmail.com

***Corresponding Author**

ABSTRACT

Strip-shaped unbonded scrap tire rubber pad isolators (SSU-STRPs), fabricated from recycled tires, have been proposed as an economical, environmentally friendly solution for seismic base isolation, particularly effective in developing countries. The study numerically investigates the behavior of strip-shaped unbonded scrap tire rubber pad isolators (SSU-STRPs) under multidirectional cyclic lateral loading with a constant axial load of 5 MPa, using finite element analysis. In order to assess the geometric anisotropy and the directional dependency, the research focuses on the isolators' hysteretic response, normalized lateral stiffness, and the effective damping values for various length-width ratios, such as the L/B ratio of 1 to 5, and loading orientations of 0°, 45°, and 90°. The cyclic response exhibits stable hysteresis behavior with the smooth force-displacement loops, and no indication of unstable behaviour in the large deformations applied laterally, indicating reliable deformation capacity. The findings indicate that the lateral stiffness is highly dependent on the level of deformation, direction of loading, as well as by the geometry configuration, while the effective damping properties are higher when the lateral deformation is greater, which is associated with a large energy dissipation strength. The findings demonstrate the effectiveness of SSU-STRP isolators as low-cost seismic base isolation components, and provide useful guidance for numerical modelling, as well as the practical use in seismic-resistant structures.

Keywords: *Strip-Shaped, Scrap tire rubber pad isolators, stiffness, damping, Multidirectional cyclic loading*

1. INTRODUCTION

Seismic isolation is the process by which structures, such as buildings and bridges, are protected by dissipating energy and flexibility. Among the various seismic base isolator, elastomeric base isolators are widely utilised. Elastomeric base isolators, which are usually made of steel and rubber layers, allow for flexibility during earthquakes while also providing a substantial vertical loading capacity that maintains stability. They are widely used in seismic base isolation systems for civil engineering because of their ability to effectively damping seismic energy and provide sufficient vertical load support (Li & Li, 2014; Nithin & Varma, 2017).

Steel-reinforced elastomeric isolators (SREIs) are one of the most popular types because of their high ability to absorb seismic energy and withstand significant displacements (Guo et al., 2025). However, SREIs are expensive to produce and unsuitable for low-income nations (Konstantinidis & Kelly, 2012; Strauss et al., 2014). Therefore, developing nations need a seismic base isolation system that is both efficient and affordable, featuring simple installation and lower production costs. Researchers have investigated a variety of isolators in recent years, including Friction Pendulum System (Lupăşteanu et al., 2019), High Damping Rubber Bearings (HDRBs) (Wang et al., 2025; Grant., 2004), and lead rubber bearings (LRBs) (Marquez et al., 2021; Lee et al., 2012). Although each of these systems has unique benefits, low-income developing nations have found them difficult to implement due to their complicated manufacturing, construction, and cost processes. In recent years, recycle materials such as scrap tire rubber are using as a base isolator. The alternative isolator known as scrap tire rubber pad isolators (STRPs) is a cost-effective and environmentally friendly seismic isolation solution that is made from recycled tires. Some researchers have shown that scrap tire rubber pads as isolators are very effective and advantageous for reducing environmental pollution as it diminishes the large stock of scrap tire that pollutes the environment (Tsompanakis et al., 2011). Numerous numerical and experimental investigations have shown how well STRP isolators function under lateral loading conditions. Some researchers investigated layer-bonded and layer-unbonded STRP isolators manufactured from Bridgestone tires (Mishra, 2012). and some measured the seismic demand of the unbonded square and strip-shaped STRP isolators and used FEM to study their performance (Zisan and Igarashi, 2021). According to their research, bonded isolators are subject to high tensile stress, which might cause them to break. In contrast, unbonded isolators are susceptible to significant deformation and slippage failure.

However, in reality very high emphasis was put on the vertical and horizontal performance of isotropic or symmetric rubber bearings under shear to less degree for the influence geometry (i.e., anisotropy) and multi-axial loadings of “strip-shaped” rubber pad isolators. In this work, a numerical model is developed for determining the lateral stiffness, and effective damping of strip shaped scrap-tire rubber pad isolators (SSU-STRP) of different L/B (length/width) ratios under horizontal cyclic loads under a constant axial load of 5 MPa. The strip shape is responsible for the geometric anisotropy of lateral responses to the loading direction compared with principal axes, which is held only when a longer length or width distance occurs on the pad. As a consequence, the horizontal stiffness and energy dissipation can be very different at 0°, at 90° (parallel to width) and also angle as 45° between them.

The motivation for the work is then evident as by modelling strip-shaped scrap-tire rubber isolators (SSU-STRP) with different aspect ratios and cyclic loading direction, the study can address a literature gap in terms of geometry driven anisotropy, and sustainable isolator design. This study is important for places like Bangladesh, which faces seismic risk and has limited budgetary resources as well as environmentally unsustainable waste production; therefore, low-cost innovation-based approaches are preferred. The research has double benefit. First, it provides for design guidelines by allowing engineers to define what the L/B and loading direction should be; in order to determine optimised horizontal stiffness and effective damping and as such enable the pad geometry to be designed with optimal isolation performance. Second, it promotes sustainable development: the achievement that recycled tire rubber pads can be properly modelled and employed under realistic

cyclic forces promotes circular reuse of waste tires to be used as engineering material and shifting away from expensive commercial isolators.

Finally, through the incorporation of geometric anisotropy, cyclic multidirectional loading, and environmentally sustainable material use, and numerical modelling work seeks to offer a pertinent design framework for strip-shaped scrap tire-rubber pad isolators (SSU-STRP) in view of effective seismic isolation performance, enhanced structural capacity by reducing seismic forces on structures, as well as environmental gain.

2. STRIP-SHAPED UNBONDED STRP MODELLING

A numerical model is developed as part of this study to determine the horizontal stiffness, and equivalent damping ratio for strip-shaped unbonded scrap tire rubber pad isolators (SSU-STRP) subjected to multidirectional cyclic horizontal loading under a 5 MPa constant axial compressive stress. The modelling scheme is aimed to research the effect of L/B ratio and loading direction on lateral dynamic response of isolator.

Finite element modelling of the SSU-STRP isolator was done using MSC Marc Mentat software. The SSU-STRP isolators were modelled in 3D with varying length to width ratio (L/B=1-5), corresponding to dimensions of 50 mm x 50 mm x 24 mm, 100 mm x 50 mm x 24 mm, 150 mm x 50 mm x 24 mm, 200 mm x 50 mm x 24 mm, and 250 mm x 50 mm x 24 mm shown in Figure 1.

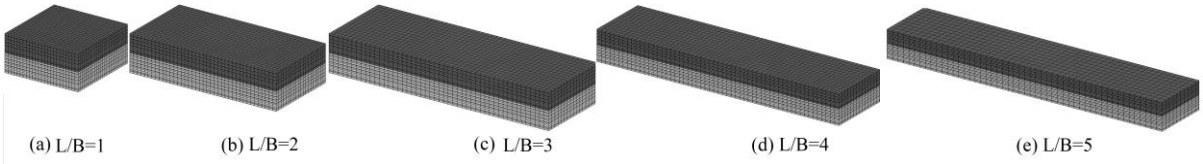

Figure 1: Variation of SSU-STRP geometry with different Length-to-Width ratios

The SSU-STRP isolator has a total thickness of 12 mm and has 5 reinforcement layers, each is ±70° with the carcass steel direction. The isolator was developed by attaching 12-mm rubber pads together to get the required geometry. Initially, the rubber matrix of the first stack T1 was modelled using carcass layers and four steel belt layers (Belt1, Belt2, Belt3, and Belt4). Figure 2 depicts the subsequent configuration of the steel cord layers, referred to as the carcass and belts 1 to 4. The complete two stack SSU-STRP isolators illustrated in Figure 3 were subsequently finished by modelling and placing another stack, T2, on the top of T1.

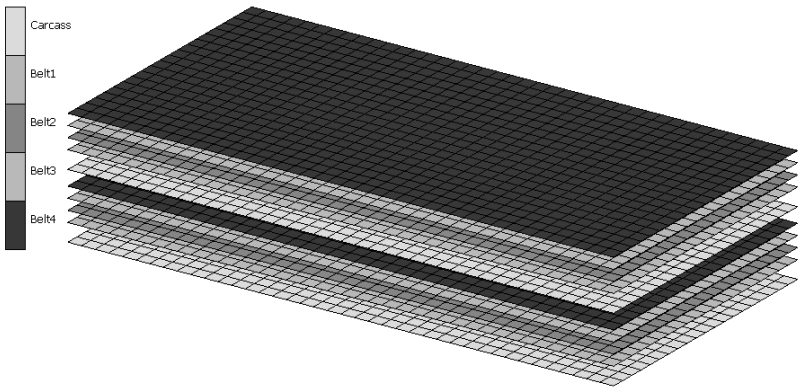

Figure 2: Modelling of Embedded steel cord

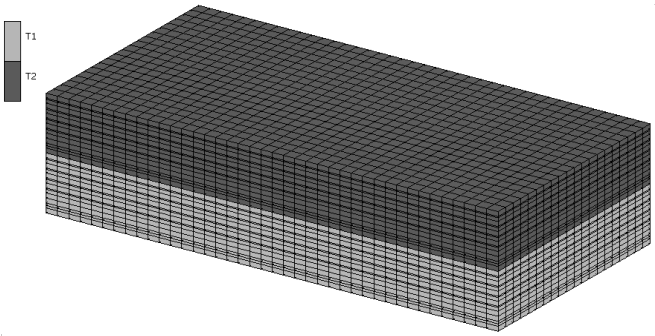

Figure 3: Strip-Shaped Unbonded (SSU-STRP) Model

3. MATERIAL MODELLING

The rubber element was modelled using Hermann type components, and the rebar was modelled using hollow isoperimetric rebar elements. The properties of the steel cord layer and rubber material have been taken from the work of Zisan and Igarashi (2021). Tables 1 and 2 provide descriptions of the material properties of steel cord and rubber chord, respectively. Two more surfaces with the labels "bottom" and "top" were sketched. The "top" surface was free to move in both directions and is sensitive to both vertical and lateral loads, but the "bottom" surface was conceived of as a fixed support. The layer bonded isolators were represented by the contact interactions between stacks T1 and T2. To represent the unbonded state, the contact interactions between the SSU-STRP isolators and the other two surfaces were based on friction. The friction coefficient between SSU-STRP and the other two surfaces was used 0.8 bilinear coulomb friction. The "top" surface was subjected to an axial load of 5 MPa and a cyclic lateral load of up to 250% shear strain. In Figure 4, the pattern of the lateral loading used in the experiment as well as the finite element analysis is displayed. The lateral movement was imposed in six cycles in six different magnitudes and thus the rubber pad was allowed to undergo as much as 250% shear deformation.

Table 1: Properties of reinforcing steel cord in a SSU-STRP isolator (Zisan & Igarashi, 2021)

Layer	No. of layer	No. of filaments	Filament diameter (mm)	Single cord area (mm^2)	Orientation	Equivalent thickness t_f (mm)	Yield strength (MPa)	Spacing (mm)	Young's modulus (GPa)	Poisson's ratio
Carcass	1	5	0.2	0.44	0°	0.40	2800	2.5	200	0.3
Belt	4	14	0.4	0.63	∓70°					

Table 2: Mooney-Rivlin material constants (Zisan & Igarashi, 2021)

Mooney-Rivlin Constant			Shear Modulus (MPa)			Prony Shear Responses				Mullin-Damage Parameters			
C_{10}	C_{01}	C_{11}	G_{eff}	G_0	v	δ^1	λ^1	δ^2	λ^2	η_1	m_1	η_2	m_2
0.40	1.22315	0.18759	1.10	1.31	0.49995	0.30	0.2	0.30	0.55	0.01	5	0.05	10

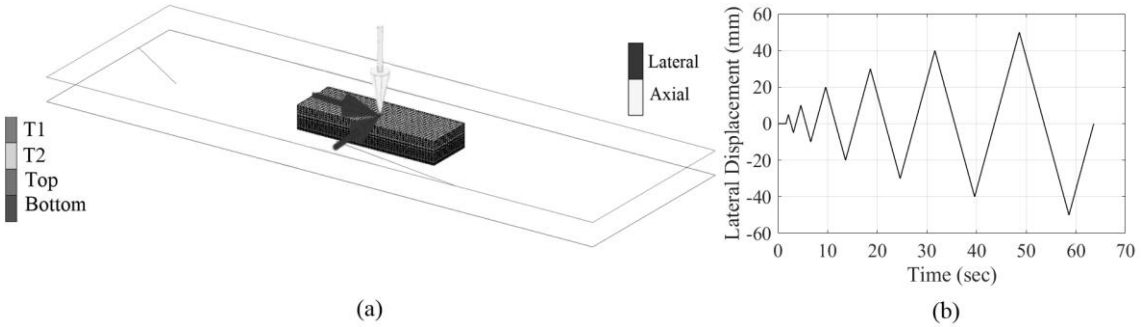

Figure 4: Model Boundary conditions and loading patterns of the SSU-STRP isolators

4. ANALYTICAL CHARACTERIZATION

The lateral stiffness (K_h) of the SSU-STRP isolator is obtained using the following equation (ASCE/SEI 7-10, 2010):

$$K_h = \frac{F^+ - F^-}{u^+ - u^-} \tag{1}$$

Here, F+ and F- are the maximum positive and negative restoring forces, respectively, whereas u+ and u- are the maximum positive and negative displacement of isolator.

Effective damping β is determined by the following equation:

$$\beta = \frac{2}{\pi}\left[\frac{E_{loop}}{K_h\left(u^+ - u^-\right)^2}\right] \tag{2}$$

Here, E_{loop} is the region bounded by the hysteresis of the force-displacement curve for the ravenous loading-cycle. This is particularly evident in the case of a base isolator, where the appropriate effective damping ratio should fall within the range of 10% to 20% as specified in Eurocode 8 (BS EN 1998-1:2004).

5. MODEL VALIDATION

The FE model is verified against the reference model of Zisan and Igarashi (2021) work. To validate the model, uniaxial cyclic loading is applied on the SSU-STRP isolator exactly the same as with the reference model, and the lateral stiffness and damping ratio are determined. From Figure 5, it can be seen that the FE model and the reference model's value have less than 5% error and match almost exactly. So, it can be said that our model is validated and can be used for further study.

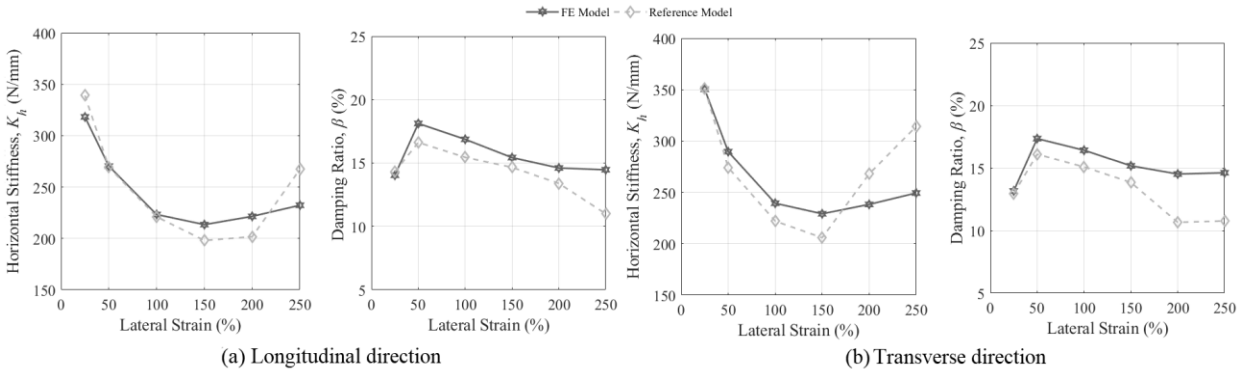

Figure 5: Model Validation

6. RESULTS AND DISCUSSION

Figure 6-8 shows the hysteresis curves of SSU-STRP isolators operating under cyclic lateral loading at 0°, 45°, and 90° loading, up to 250% lateral strain. Hysteresis response of all variations shows rollover behaviour with smooth and steady force-displacement loops at least to 200% lateral strain without any sudden change or instability. The findings demonstrate that under 0° loading, the normalized load at 200% lateral strain rises with L/B; however, the normalized load only increases by roughly 92% when comparing the SSU-STRP with L/B = 1 to L/B = 5. Similarly, for under 45° loading, the normalized load at 250% lateral strain increases somewhat in the same direction with an

increase in L/B, specifically between 1.8 and 2.2, increasing by roughly 22.2% at L/B of 1 to 5, respectively. On the contrary, under 90° loading, the normalized load at 250% lateral strain does not vary significantly at both L/B = 1 to L/B = 5, meaning it does not change significantly as the L/B ratio varies.

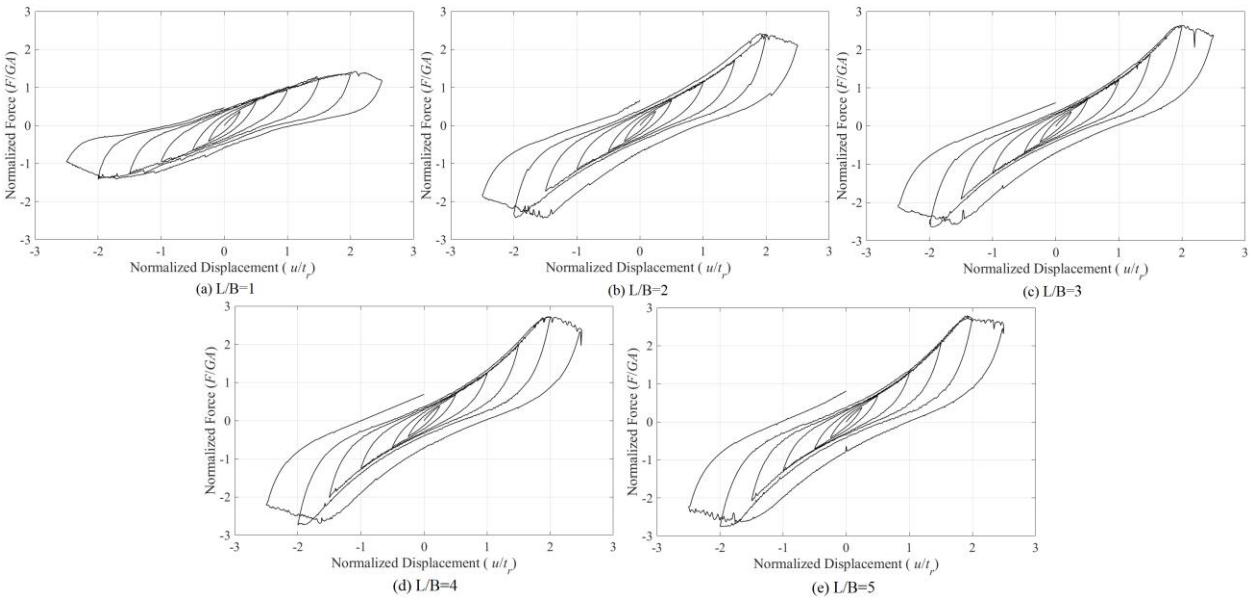

Figure 6: Hysteresis Curve for Cyclic Lateral Load at 0°

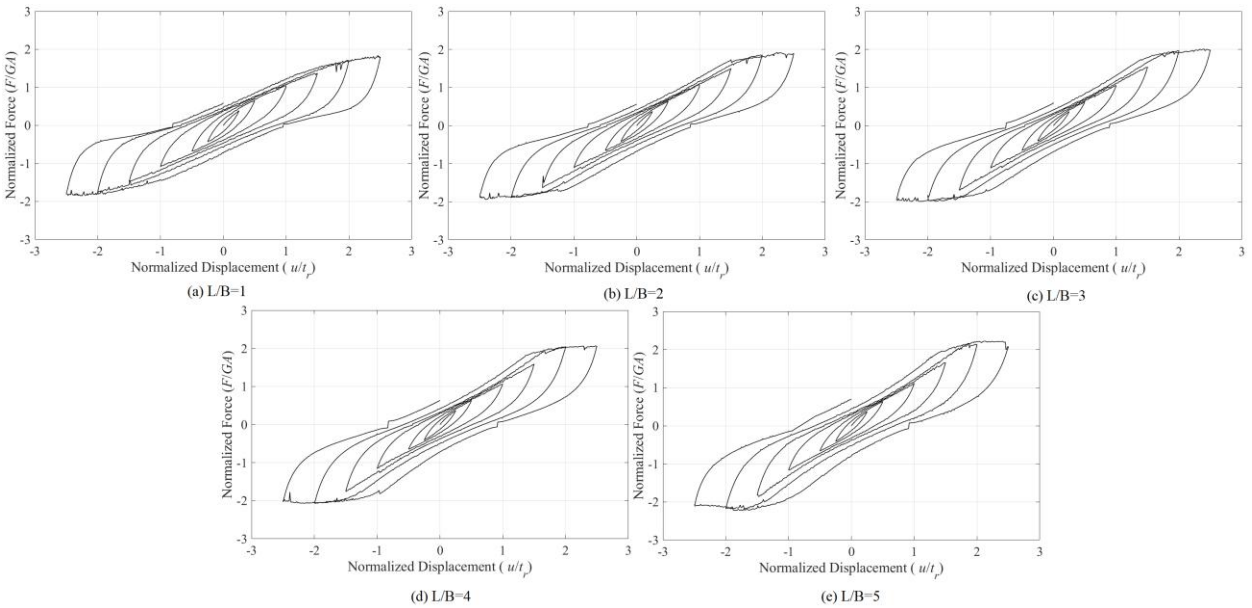

Figure 7: Hysteresis Curve for Cyclic Lateral Load at 45°

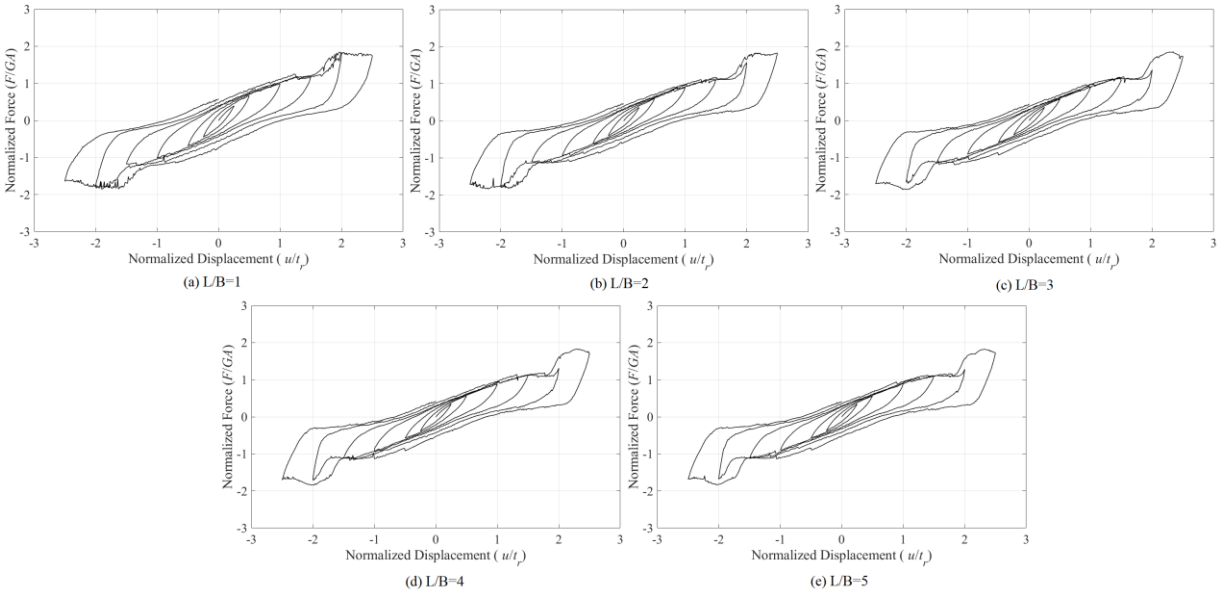

Figure 8: Hysteresis Curve for Cyclic Lateral Load at 90°

6.1 STIFFNESS

Table 3-5 shows the normalized lateral stiffness values of SSU-STRP isolators at varying loading direction that are estimated from hysteresis curves using Eqn. (1). Table 3, shows normalized lateral stiffness, $(K_h t_r/GA)$ of the SSU-STRP isolators in 0° loading at different normalized lateral strains and at varied L/B ratios. The lateral stiffness is high at lower lateral strains (0.25 and 0.50) and at all the ratios of L/B. If the normalised lateral strain is 0.25, the typical stiffness in the range of 1-5 L/B ratio is 1.58-1.60. The stiffness can be seen to decrease considerably as the lateral strain rises to 1.00 and above. Precisely, individual values of stiffness reduce to 0.57-1.07 at a normalized lateral strain of 2.5 0 in relationship to the L/B ratio. Table 4, illustrates the normalized lateral stiffness at 45° loading of SSU-STRP isolators. The same trends can be observed although the values of stiffness are normally less than at 0 loading. The stiffness values at normalized lateral strain of 0.25 vary between 1.15 (L/B = 4) and 1.68 (L/B = 1). The values of stiffness keep on reducing as the lateral strain is increased. At 2.50 normalized lateral strain, the values fall within the range of 0.60 and 0.89, based on L/B ratio. Table 5 shows the normalized lateral stiffness under 90° loading, the values of which are lower than at 0° or 45° loading conditions. The stiffness values 1.46 to 1.68 with greatest values occurring at L/B = 1 at 0.25 normalized lateral strain. The stiffness further decreases with increase in the lateral strain. Indicatively, when the lateral strain is normalized to 2.50, the values of the normalized lateral stiffness range between 0.73 and 0.74 and there is a minor variation among the L/B ratios. Figure 9, illustrates the lateral stiffness of SSU-STRP isolators at varying loading conditions.

Table 3: Normalized Lateral Stiffness, $(K_h t_r/GA)$ of SSU-STRP isolators at 0° Loading

Normalized Lateral Strain (u/t_r)	L/B=1	L/B=2	L/B=3	L/B=4	L/B=5
0.25	1.58	1.59	1.59	1.62	1.60
0.50	1.28	1.33	1.38	1.37	1.40
1.00	0.95	1.15	1.22	1.24	1.29
1.50	0.82	1.15	1.26	1.33	1.38
2.00	0.69	1.21	1.31	1.36	1.39
2.50	0.57	0.97	1.04	1.08	1.07

Table 4: Normalized Lateral Stiffness, $(K_h t_r/GA)$ of SSU-STRP isolators at 45° Loading

Normalized Lateral Strain (u/t_r)	L/B=1	L/B=2	L/B=3	L/B=4	L/B=5
0.25	1.68	1.58	1.15	1.55	1.57
0.50	1.35	1.30	0.97	1.28	1.30
1.00	1.00	1.10	0.81	1.11	1.14
1.50	0.80	1.05	0.81	1.12	1.17
2.00	0.92	0.94	0.74	1.03	1.09
2.50	0.74	0.77	0.60	0.83	0.89

Table 5: Normalized Lateral Stiffness, $(K_h t_r/GA)$ of SSU-STRP isolators at 90° Loading

Normalized Lateral Strain (u/t_r)	L/B=1	L/B=2	L/B=3	L/B=4	L/B=5
0.25	1.68	1.53	1.49	1.47	1.46
0.50	1.35	1.22	1.16	1.14	1.13
1.00	1.00	0.92	0.91	0.91	0.90
1.50	0.80	0.75	0.77	0.77	0.74
2.00	0.92	0.84	0.77	0.76	0.74
2.50	0.74	0.73	0.74	0.73	0.73

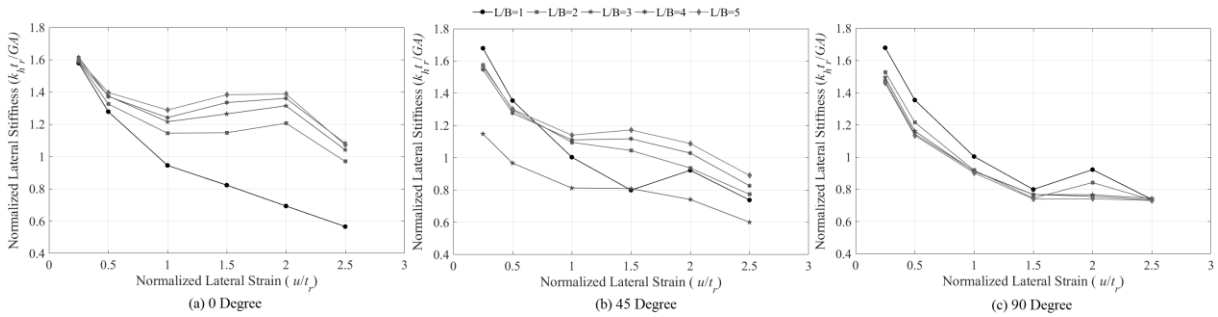

Figure 9: Lateral Stiffness of SSU-STRP isolators at varying loading conditions

6.2 EFFECTIVE DAMPING

Table 6-8 shows the effective damping ratio, β (%) values of SSU-STRP isolators at varying loading direction that are estimated from hysteresis curves using Eqn. (2). Table 6 illustrates that the damping ratio in the 0° loading scenario goes up with the lateral strain at all the ratios of L/B. At a normalized lateral strain of 0.25, β (%) varies between 11.29% to 13.49% whereas at 2.50, the damping ratios are much higher ranging between 18.47% to 22.35%. The same strain increment tendency is seen in 45° loading (Table 7), in which β (%) increases with strain 11.59-13.30% at 0.25 strain to 19.72-20.13% at 2.50 strain. This suggests that there is more energy dissipation ability when the deformations are large. At loads under 90° (Table 8), the ratios of the damping are similar but slightly lesser at a higher L/B ratio. As illustration, at 0.25 strains the β (%) values lie between 11.91% to 13.30%, whereas at 2.50 strain β (%) values go up to 16.61-20.00%. According to Eurocode 8, Rubber-based isolation systems are allowed to have damping ratios between 10% and 20%. Turer and Özden (2007) reported that scrap tire rubber demonstrates a relatively high damping ratio, typically varying between 18% and 22%, which makes it suitable for vibration and seismic isolation applications. Therefore, damping ratios obtained between 11% and 22% at all loading orientations demonstrate excellent damping performance. Besides, the findings indicate that those isolators with low L/B ratios tend to give higher damping at all loading angles and all levels of deformation implying higher energy dissipation because of the high deformation capacity. Figure 10, give β (%), the values of effective damping ratios of SSU-STRP isolators under the conditions of 0°, 45°, and 90° loading.

Table 6: Effective Damping ratios, β (%) of SSU-STRP isolators at 0° Loading

Normalized Lateral Strain (u/t_r)	L/B=1	L/B=2	L/B=3	L/B=4	L/B=5
0.25	13.49	11.89	11.35	11.13	11.29
0.50	17.29	14.50	13.10	13.55	13.60
1.00	18.10	13.59	12.69	12.39	12.11
1.50	17.68	12.12	11.04	10.61	10.39
2.00	19.54	11.81	11.30	11.29	11.58
2.50	22.35	18.17	17.60	17.67	18.47

Table 7: Effective Damping ratios, β (%) of SSU-STRP isolators at 45° Loading

Normalized Lateral Strain (u/t_r)	L/B=1	L/B=2	L/B=3	L/B=4	L/B=5
0.25	13.30	11.59	11.84	10.47	11.70
0.50	17.19	15.21	12.53	14.53	14.54
1.00	17.72	14.58	14.05	13.63	13.58
1.50	18.51	13.91	13.26	12.80	12.48
2.00	15.78	15.86	15.28	14.98	14.74
2.50	20.00	19.72	19.77	19.38	20.13

Table 8: Effective Damping ratios, β (%) of SSU-STRP isolators at 90° Loading

Normalized Lateral Strain (u/t_r)	L/B=1	L/B=2	L/B=3	L/B=4	L/B=5
0.25	13.30	12.35	12.19	11.97	11.91
0.50	17.19	15.80	15.80	15.61	15.45
1.00	17.72	16.02	15.32	15.08	14.89
1.50	18.51	16.82	15.77	15.37	15.65
2.00	15.78	14.59	15.31	15.10	15.12
2.50	20.00	17.64	16.86	16.71	16.61

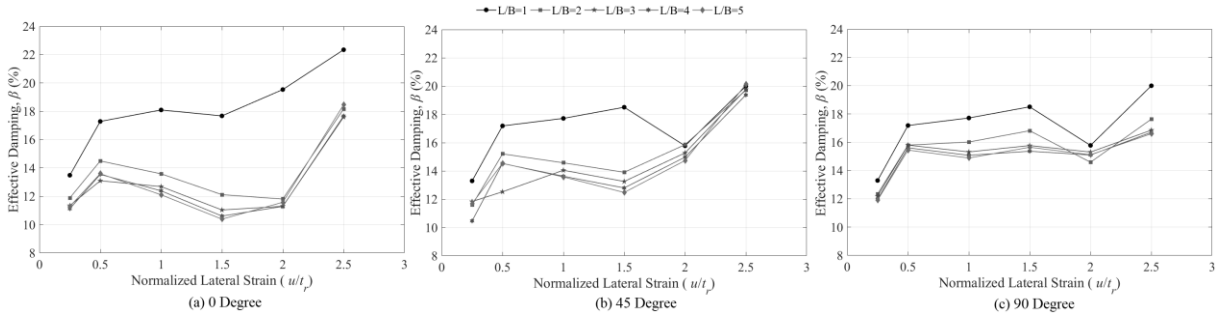

Figure 10: Effective Damping of SSU-STRP isolators at varying loading conditions

7. CONCLUSIONS

The study provides the lateral load behaviour of strip-shaped unbonded scrap tire pad isolators (SSU-STRPs) under cyclic lateral loading based on the finite element analysis study. The study focused on the hysteresis response, normalized lateral stiffness, and effective damping ratios at different L/B ratios and loading orientations.

- Hysteresis response of SSU-STRP isolators, rollover behaviour has been observed to be stable, exhibiting a smooth and steady force-displacement loop to approximately 200% lateral strain with no abrupt change or instability. At 0° loading, the normalized load at 200% lateral strain rises with the L/B ratio, and it rises approximately 92% as the length/width ratio increases from 1 to 5. In the same way, for under 45° loading, the normalised load at 250% lateral strain increases somewhat in the same direction with an increase in L/B, notably between 1.8 and

2.2, and increases by about 22.2% for L/B of 1 to 5, respectively. There is relatively no effect of L/B ratio on normalized load at 250% lateral strain under 90° loading.

- The findings show that the normalized lateral stiffness of the SSU-STRP isolators draws a direct negative relation to the increase in lateral strain in all directions of loading and the L/B ratios. At lower deformation levels (0.25-0.50 u/t_r), the stiffness is comparatively large, and its sharp decrease is noticed with the strain increasing to 1.00 and more. The highest values of the stiffness are observed in the 0° orientation and then in 45° and minimum at 90°. Moreover, the isolators with smaller L/B ratios will always be more rigid at all levels of strain, which proves that small plan dimensions in comparison to the thickness confer a high level of lateral rigidity.

- The findings also show that all loading directions and geometries exhibit the same pattern: the damping ratio of SSU-STRP isolators increases with the applied strain in the lateral plane as the plane load increases. Effective damping ratio at small deformations (0.25 u/t_r) is between 11.29% to 13.49% to large deformations (2.50 u/t_r) giving 18.47% to 22.35% respectively, a sign of increased energy loss with strain. As much as the damping of 0° and 45° loading is a little higher than that of 90° loading, there is a small difference which indicates that it performs well in all loading directions. Isolators that are smaller in L/B ratios always exhibit evidence of a higher damping, which is indicative of a higher ability of the isolators to absorb energy owing to their greater ability to deform.

REFERENCES

ASCE/SEI 7-10 (2010), Minimum Design Loads for Buildings and Other Structures, ASCE, 1801 Alexander Bell Drive, Reston, Virginia, USA

Eurocode 8 (2004), Design of Structures for Earthquake Resistance, BS EN 1998-1:2004

Grant, D. N., Fenves, G. L., & Auricchio, F. (2004). Bridge isolation with high-damping rubber bearings: Analytical modelling and system response. In Proceedings of the 13th World Conference on Earthquake Engineering (13WCEE), Vancouver, Canada, August 1–6. Paper No. 1002.

Guo, K., Pianese, G., Valente, M., Pan, P., & Milani, G. (2025). Experimental and numerical investigation of elastomeric seismic isolators coupled with S-shaped steel dampers. Structures. https://doi.org/10.1016/j.istruc.2025.109472

Konstantinidis, D., & Kelly, J. M. (2012). Two low-cost seismic isolation systems. In Proceedings of the 15th World Conference on Earthquake Engineering (15WCEE), Lisbon, Portugal.

Lee, H. P., Cho, M. S., & Park, J. Y. (2012). Developing lead rubber bearing for seismic isolation of nuclear power plants. In Proceedings of the 15th World Conference on Earthquake Engineering (15WCEE), Lisbon, Portugal.

Li, Y., & Li, J. (2014). Base isolator with variable stiffness and damping: Design, experimental testing and modelling. In S. T. Smith (Ed.), Proceedings of the 23rd Australasian Conference on the Mechanics of Structures and Materials (ACMSM23) (Vol. 2, pp. 913–918). Southern Cross University, Lismore, NSW. https://creativecommons.org/licenses/by/4.0/

Lupășteanu, V., Soveja, L., Lupășteanu, R. & Chingălată, C. (2019). Installation of a base isolation system made of friction pendulum sliding isolators in a historic masonry Orthodox church. Engineering Structures, 188, 369-381. https://doi.org/10.1016/j.engstruct.2019.03.040

Marquez, J. F., Mosqueda, G., & Kim, M. K. (2021). Modeling of Lead Rubber Bearings under Large Cyclic Material Strains. Journal of Structural Engineering, 147(11). https://doi.org/10.1061/(asce)st.1943-541x.0003151

Mishra HK (2012), "Experimental and Analytical Studies on Scrap Tire Rubber Pads for Application to Seismic Isolation of Structures" PhD Thesis, Kyoto University, Japan.

Nithin, A. V., & Varma, A. P. (2017). *Seismic base isolators under individual and combined use in multi-storied buildings – A review*. *International Research Journal of Engineering and Technology (IRJET)*, 4(2), 1232–1236. Retrieved from https://www.irjet.net

Strauss, A., Apostolidi, E., Zimmermann, T., Gerhaher, U., & Dritsos, S. (2014). Experimental investigations of fiber and steel reinforced elastomeric bearings: Shear modulus and damping coefficient. Engineering Structures, 75, 402–413. https://doi.org/10.1016/j.engstruct.2014.06.008

Tsompanakis, Y., Psarropoulos, P., & Drosos, V. (2011). Low-cost seismic base isolation using recycled tire cushions. In Proceedings of the Thirteenth International Conference on Civil, Structural and Environmental Engineering Computing. Civil-Comp Press. https://doi.org/10.4203/ccp.96.70

Turer A and Özden B (2007), "Seismic Base Isolation Using Low-Cost Scrap Tire Pads (STP)," Materials and Structures, 41(5): 891–908.

Wang, B., Niu, Q., Chen, P., Zhang, Z. & Karavasilis, T.L. (2025). Experimental and numerical investigations on mechanical properties of high-damping rubber bearings under large strain loading. Construction and Building Materials, 140390. https://doi.org/10.1016/j.conbuildmat.2025.140390

Zisan, M. B., & Igarashi, A. (2021). Lateral load performance evaluation of unbonded strip-STRP base isolator. https://doi.org/10.1007/s11803-021-2053-4